CCFE
CULHAM CENTRE FOR FUSION ENERGY

UK Atomic Energy Authority

UKAEA-CCFE-PR(22)22

P. J. Bonofiglo, V. Kiptily, V. Goloborodko, Z. Stancar, M. Podesta, F. E. Cecil, C. D. Challis, J. Hobirk, A. Kappatou, E. Lerche, I. Carvalho, J. Garcia, J. Mailloux, C. F. Maggi, A. G. Meigs

Lost Alpha Faraday Cup Foil Noise Characterization During JET Plasma Post-Processing Analysis

Lost Alpha Faraday Cup Foil Noise Characterization During JET Plasma Post-Processing Analysis

P. J. Bonofiglo, V. Kiptily, V. Goloborodko, Z. Stancar, M. Podesta, F. E. Cecil, C. D. Challis, J. Hobirk, A. Kappatou, E. Lerche, I. Carvalho, J. Garcia, J. Mailloux, C. F. Maggi, A. G. Meigs

This is a preprint of a paper submitted for publication in Review of Scientific Instruments

Lost Alpha Faraday Cup Foil Noise Characterization During JET Plasma Post-Processing Analysis

P. J. Bonofiglo,[1, a)] V. Kiptily,[2] V. Goloborodko,[3] Z. Stancar,[2, 4] M. Podestà,[1] F. E. Cecil,[5] C. D. Chalis,[2] J. Hobirk,[6] A. Kappatou,[6] E. Lerche,[2, 7] I. Carvalho,[8] J. Garcia,[9] J. Mailloux,[2] C. F. Maggi,[2] A. G. Meigs,[2] and JET Contributors[b)]

[1)] *Princeton Plasma Physics Laboratory, Princeton, NJ, USA*
[2)] *Culham Centre for Fusion Energy of UKAEA, Culham Science Centre, Abingdon, United Kingdom*
[3)] *Kyiv Institute for Nuclear Research, Kyiv, Ukraine*
[4)] *Josef Stefan Institute, Slovenia*
[5)] *Colorado School of Mines, Golden, CO 80401, USA*
[6)] *Max-Planck-Institut für Plasmaphysik, Garching, Germany*
[7)] *LPP-ERM-KMS, Association EUROFUSION-Belgian State, TEC Partner, Brussels, Belgium*
[8)] *Instituto de Plasmas e Fusão Nuclear, Instituto Superior Técnico, Universidade de Lisboa, Lisbon, Portugal*
[9)] *CEA-IRFM, Saint Paul Lez Durance, France*

(Dated: 30 April 2022)

Capacitive plasma pickup is a well-known and difficult problem for plasma-facing edge diagnostics. Ths problem must be addressed to ensure an accurate and robust interpretation of the real signal measurements versus noise. JET's Faraday cup fast ion loss detector array is particularly prone to this issue and can be used as a testbed to prototype solutions. The separation and distinction between warranted fast ion signal and anomalous plasma noise has traditionally been solved with hardware modifications, but a more versatile post-processing approach is of great interest. This work presents post-processing techniques to characterize the signal noise. While hardware changes and advancements may be limited, the combination with post-processing procedures allows for more rapid and robust analysis of measurements. The characterization of plasma pickup noise is examined for alpha losses in a discharge from JET's tritium campaign. In addition to highlighting the post-processing methodology, the spatial sensitivity of the detector array is also examined which presents significant advantages for the physical interpretation of fast ion losses.

I. INTRODUCTION

With JET's recent 2021 tritium and deuterium-tritium campaign, energetic alpha particle experiments have found a resurgence.[1–3] New studies concerning alpha particle confinement, heating, mode destabilzation, etc. have been performed on JET.[4,5] Such experiments may become more commonplace as fusion pilot plants are being developed, the construction of ITER nears completion, and private enterprises are rapidly pushing towards reactor relevant plasmas. One of the key measurements from these studies is that of fast ion losses.

Fast ion loss detectors (FILDs) have become ubiqutous in magnetic confinement experiments.[6–11] FILDs can provide quantitative measurments of energetic particle losses to validate transport models and directly confer fast ion activity.[12] Faraday cup fast ion loss detectors utilize thin metal foils to measure lost fast ion current.[13–16] Compared to scintillator probes [17], Faraday cups offer a simple engineering design and low construction costs which permits the installation of entire arrays across the machine vessel.

JET contains an array of Faraday cup FILDs which poloidally span the outboard side of the machine from near the midplane to approximately the divertor region.[7] The Faraday cups are pre-assembled into five "pylons" which may house up to three cups across a small radial extent. This design covers a broad region of the outboard wall and can provide spatial information on fast ion loss footprints. Additionally, each Faraday cup is composed of four alternating laters of thin Ni foil and insulating mica which can provide a rough energy resolution for a given incident lost ion. A full description and image of the entire diagnostic array can be found in references [7] and [12].

The chaotic environment of fusion plasmas, however, makes the interpretation of Faraday cup signals very difficult since the detectors are, essentially, just floating pieces of metal. The Faraday cup FILDs are plasma facing and are susceptible to multiple noise sources which can produce anomalous currents within the foil.[14,18,19] As such, differentiating the true lost ion signal from any plasma coupling poses a challenging problem.

JET's Faraday cup FILD array has been shown to suffer from strong plasma coupling as the foil-insulator stack effectively makes a stack of capacitors.[16,20] The plasma can couple to the front-foil and propagate through the stack capacitively. This problem may be remedied with hardware solutions: install a grounded front-foil, build

[a)] Electronic mail: pbonofig@pppl.gov
[b)] See the author list of E. Joffrin et al. 2019 Nucl. Fusion **59** 112021

a "dummy" Faraday cup for pure noise measurements, or add Langmuir or capacitive probes to infer the local electric field. New hardware implementations, however, complicate the diagnostic design and, more importantly, require machine access. In addition to extended experimental campaigns, the radiological hazard imposed by tritium fuel limits personnel access and hardware modifications. This was the case for JET's recent tritium and deuterium-tritium campaign where no diagnostic modifications could be made. Therefore, it is advantageous to seek a purely post-processing approach to filter and mitigate any Faraday cup noise.

This paper discusses a general methodology for obtaining pure alpha loss measurements from JET's Faraday cup FILD array while accounting for capacitive plasma pickup during post-shot analysis. The FILD signals are post-processed from their original form by utilizing spectral methods and a new corrective foil signal. The approach is discussed in Section II and applied to a JET tritium discharge in Section III. The manuscript will conclude by considering the efficacy of the post-processing analysis method and suggestions for further improvements.

II. POST-PROCESSING METHODOLOGY

The analysis procedure focuses on low frequency magnetohydrodynamic (MHD) modes which have been shown to exhibit strong losses in the Faraday cup array.[20] In particular, modes which can be spectrally decomposed in frequency-space as a function of time (kinks, neoclassical tearing modes, fishbone modes, low frequency Alfvén eigenmodes, etc.) support more sophisticated analysis techniques.

Figure 1 presents the external heating and magnetic spectrogram for JET discharge 99151 from the recent tritium campaign (I_p = 2.2 MA, B_0 = 3.4 T, n_e =7x10^{19} m^{-3}, T_e = 8.5 keV). The shot is 95% tritium with a small fraction of hydrogren for minority RF-heating. The neutral beams are fueled with tritium resulting in TT beam-thermal fusion reactions. The edge magnetic coil shows a variety of MHD activity at varying frequencies and toroidal mode numbers, n, throughout the sustained heating period. Energetic tritons produced from ion cyclotron resonance heating (ICRH) and neutral beam injection (NBI) as well as TT-fusion alpha particles can resonantly interact with these modes, undergo transport, and be lost. These losses are measureable on JET's fast ion loss detectors.

Figure 2 displays the spectrograms produced from one of JET's Faraday cup FILD foils and scintillator probe FILD [17] photomultiplier tubes (PMTs). The Faraday foil is taken from the vertical most pylon, third radial cup (closest to the wall), and fourth (bottom most) foil within the foil stack. The magnetic features shown in 1 (b.) are clearly evident in the Faraday foil. Since the various modes can capactively couple thermal plasma to the foil stack, the signal shown is most-likely a combination of actual fast ion losses and plasma coupling noise.

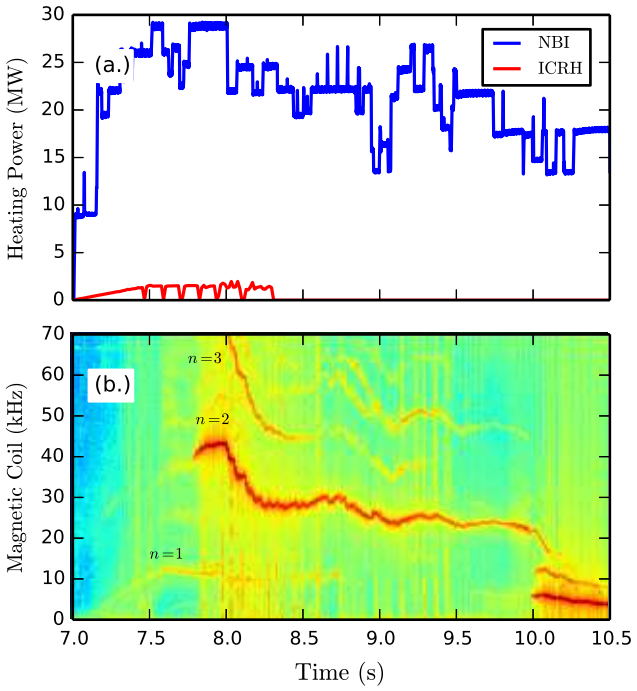

FIG. 1. External heating power, (a.), and a spectrogram from an edge magnetic Mirnov coil, (b.) for JET tritium discharge 99151. The toroidal mode numbers are identifited in subplot (a.) for $n = 1 - 3$ for the observed modes.

Scintillator probe FILDs, however, do not suffer from the anomalous currents that Faraday cup FILDs do and may serve to confirm the presence of lost energetic particles. The scintillator probe FILD signal in subplot (b.) shows fast ion losses coherent with the $n = 2$ mode from about 7.8-8.5s. The scintillator probe measurements verify that the signal detected in the Faraday foils is indeed composed of some fraction of loss energetic ions.

Since the $n = 2$ mode exhibits losses, it would be beneficial to extract this mode feature from the total Faraday foil signal. Many feature finding tools exist to find distinct features within spectrograms with varying degrees of sophistication.[21] For the purposes of this work, it is almost always possible to find at least one Faraday foil (there are a total of 44) with relatively clean features and reduced spectral noise. Figure 2 (b.) presents such an example. The $n = 2$ mode can easily be extracted by specifying a threshold amplitude value within a given time and frequency.

Figure 3 displays the $n = 2$ mode feature shown in Figure 2 found from the Faraday foil signal in subplot (b.). The mode is highlighted in red and denotes the corresponidng frequencies as a function of time that translate to a coherence with the $n = 2$ mode. The mode's time and frequency variation is well captured. The Faraday foils are all digitized at the same rate, so that the foil spectrograms can be produced with the same rolling window size. This ensures that once the location of the mode feature is found from any of the foils, then the extracted

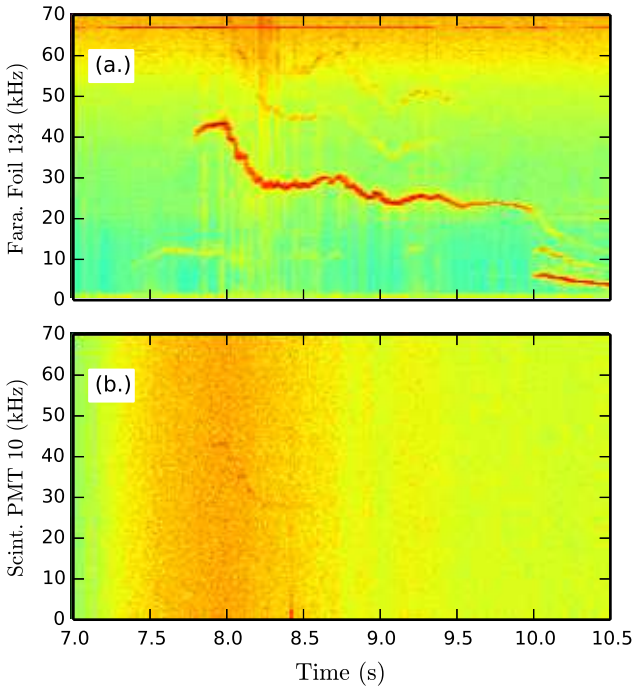

FIG. 2. Spectrogram produced from Faraday cup FILD foil 134 (first pylon, third radial cup, fourth foil), (a.), and PMT 10 from the scintillator probe FILD, (b.).

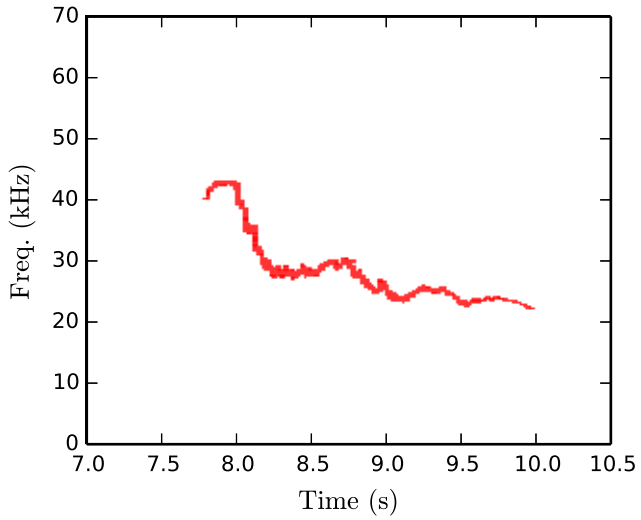

FIG. 3. The $n = 2$ mode feature extracted from the Faraday cup foil spectrogram shown in Figure 2 (a.).

structure can be used on all of the foils. Once the coherent signal for any given mode is found, any other modes present, both coherent and non-coherent, can simply be ignored. This narrows the analysis, and measured signal, down to a specific mode of interest.

Once the loss mechanism (i.e. the $n = 2$ mode) has been identified and located in frequency space, then the signal and noise need to be deconstructed. In previous work, the front-most plasma facing foil was used to correct foils deeper within a respective stack.[20] The underlying assumption was that the front-most foil would experience the strongest plasma coupling, so subtracting the front foil signal from deeper foils would remove the strongest noise components. Meaurements under vacuum showed that the foil-to-foil capacitance remained consistent across Faraday cups at a few nA, so the equal subtraction across all foils was deemed acceptable. This procedure, though, will also discount real fast ion loss signal present in the front foil which may contain losses attributed from beam-born ions and RF and fusion slowing populations. These loss populations may be appreciable in number and may overcorrect when taking the difference in foil signals.

Instead, focus is placed on the deepest Faraday foil within the stack which captures high energy ions. The deepest foil (fourth Ni layer) is susceptible to 5.6-6.35 MeV alphas and 2.0-2.25 MeV tritons. These are relatively high energies even for energetic particles. The required triton energy is much greater than the beam injection energy (∼100 keV) and represents a small fraction of ions on the RF-heated tail. Likewise, the needed alpha particle energy is much higher than the distribution created from TT beam-thermal fusion.

Figure 4 presents the normalized alpha particle distribution as a function of energy calculated from TRANSP/NUBEAM [22] at t=8.1s for pulse 99151. The

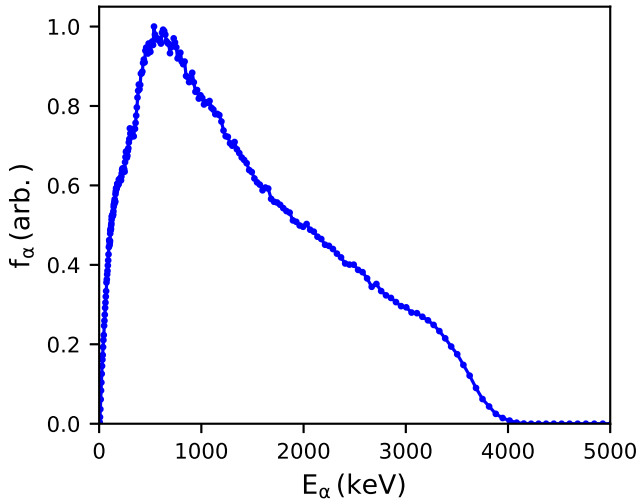

FIG. 4. The normalized alpha energy distribution as computed from TRANSP for JET shot 99151 at 8.1s.

distribution peaks around 500 keV and falls off for higher energies. This is expected as most of the fusion interactions are dominated by the beam-born ions and is in good agreement with nuclear database tables.[23] Clearly, the distribution has approched zero for alpha energies above 5 MeV. These high energy alphas can only come from fusion interactions with tritons far along the RF-heated tail which is vanishiingly small. Since the fourth Faraday cup foil is only capable of measuring 5.6-6.35 MeV alpha particles, it can be safely assumed that the foil should be

absent of any lost alpha particle signal. Therefore, any remaining lost ion signal can only come from 2.0-2.25 MeV tritons. The NUBEAM [24] and TORIC [25] codes can model the RF-heating effect but often require a substantial number of statistics to model the RF-tail out to energies in excess of 1 MeV.[12] Additionally, functional forms for the RF heating distribution function decrease exponentially with energy.[26,27] As such, any actual lost triton signal to the fourth foil can be taken as small and negligible.

It has to be stated that the assumptions made in the previous paragraph may not always hold. In advanced heating scenarios, it has been shown that alpha populations at high energies, 4-6 MeV, exist.[28] Likewise, the birth energy of DT alphas at 3.5 MeV only requiries a moderate amount of additional RF acceleration to approach the energy threshold needed to record fourth foil losses. Alfvén eigenmodes can be destabilized in JET plasmas with RF heating as well, so a super-Alfvénic RF-tail population is at least present.[29] Thus, while the fourth foil may contain some real fast ion loss signal, the loss populations are often orders of magntiude less than those present in the first foil which is susceptible to beam losses and slowing populations. In short, while the first foil may contain the strongest plasma coupling, it also contains expected heavy loss signal while the fourth foil acts in the opposite manner with weaker real signal.

In summary, after a discharge occurs and a mode of interest is determined and visible on the Faraday foils, then the mode feature can be extracted from a foil in frequency and time space. This domain specifies the mode resonant losses. The fourth, and deepest foil, is then used as a corrective factor against the other foils within a respective stack. The mode feature domain of the fourth foil is subtracted against the same domain within the other foils, and the final signal is integrated to achieve the net fast ion loss current.

III. RESULTS

The procedure outlined in Section II was applied to JET discharge 99151 for the observed $n = 2$ mode highlighted in Figure 3. Figure 5 presents the integrated foil currents for the Farady cup at the topmost pylon (pylon 1) and radial cup closest to the wall (cup 3). The signals are shown using two post-processing methodologies: utilizing the $n = 2$ spectral feature in Figure 3 and subtracting the fourth foil signal from all foils (blue squares) and band-pass filtering around the $n = 2$ mode from 20-50 kHz and subtracting the first foil signal from all foils (green triangles). Clearly, the error bars on the old method of band-pass filtering and subtracting the front foil are very large. Simply smoothing and applying a band-pass filter is too crude and does not easily acccount for the varied temporal dynamics evident in the mode. The feature finding method exactly captures the mode evolution and completely eliminates other coherent and non-coherent signal components. This reduces the error bars greatly. The individual foil signals are quite small,

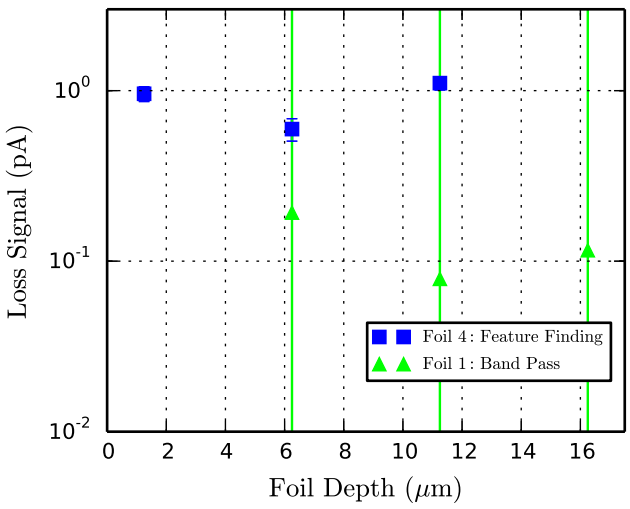

FIG. 5. Foil currents for the most vertical pylon and radial cup closest to the wall for JET pulse 99151 as a function of foil depth. Blue squares represent the spectral feature method with fourth foil correction while green triangles denote the bandd-pass filtering method with first foil correction.

pA scale, so the removal of noise and error bar reduction is critical.

Examining the spatial dependence, poloidally and radially, provides further insights to the two methodologies. The cumulative signal as function of poloidal angle below the midplane, i.e pylon, is plotted in Figure 6. Again, the blue squares denote the feature finding method using foil 4 as a corrective signal and the gren triangles represent band-pass filtering using the foil 1 signal as a corrective factor. The band-pass filtering produces very

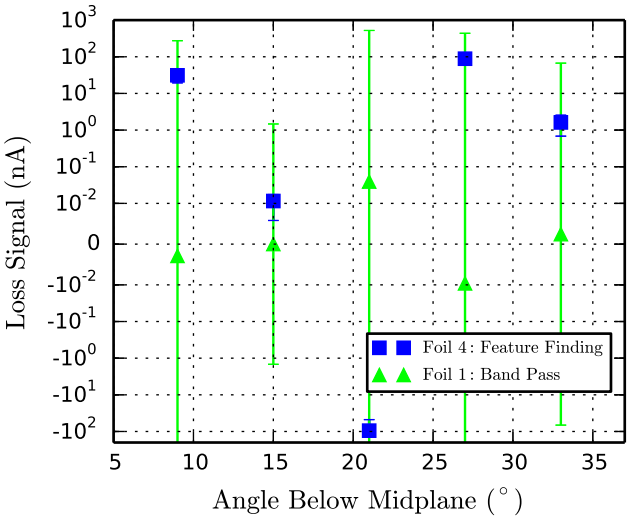

FIG. 6. Foil currents as a function of poloidal angl below the midplane (pylon) for pulse 99151. Blue squares represent the spectral feature method with fourth foil correction while green triangles denote the bandd-pass filtering method with first foil correction.

large uncertainties. Many of the foil 1 corrected signals

are also below zero which indicates that subtracting the foil 1 signal is overcorrecting the noise. That is, the total foil 1 signal, real and capacitive, is larger than the total signal of the other foils such that the correction completely eliminates and real loss signature. Thus, the corrected values are near zero, often negative, and contain large error. The high energy dependency of foil 4, however, mitigates any overcompensation of real loss signal while maintaining a good measure of the capacitive pickup.

The radial distribution of losses for the fourth pylon (27° below the midplane) is shown in Figure 7. For reference, the fourth pylon is located at $\sim R = 3.8$ m and each cup is about 2.5 cm apart. The negative signals clearly

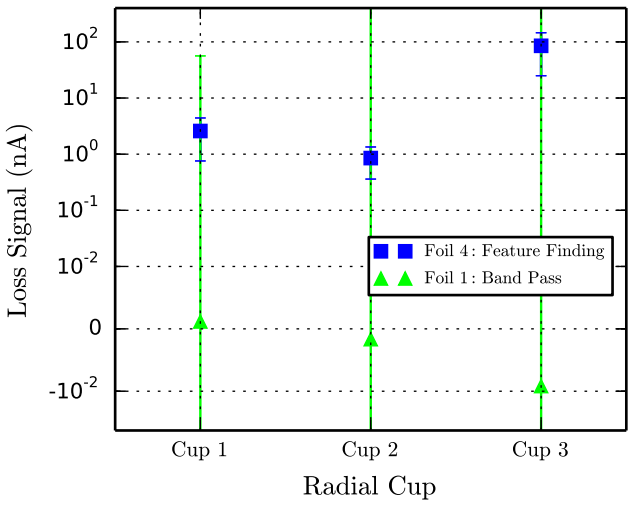

FIG. 7. Foil currents as a function of radial Faraday cup for pylon 4 (27° below the midplane) for pulse 99151. Blue squares represent the spectral feature method with fourth foil correction while green triangles denote the band-pass filtering method with first foil correction.

show an overcorrection using the front-foil. The new feature finding method with fourth foil correction shows total cup signals at about 1-90 nA which is in good agreement with estimated losses. The neutron rate is used as a proxy for alpha particle production. Integrating over the $n = 2$ mode existence gives a total of $\sim 1.9 \times 10^{19}$ neutrons. The areal fraction of the detector (A_{FILD}/A_{wall} where A_{FILD} is the total aperture area and A_{wall} is the total vessel wall area) is about $5.42{\times}10^{-6}$. Assuming isotropic losses of alphas on the vessel wall (not an entirely true assumption based on the transport properties at hand) and a reasonable loss fraction of $2 - 10\%$, gives a total loss current of 640-3200 nA or 40-210 nA per Faraday cup assuming an even distribution among the cups. These values likely serve as maximums considering this assumes an even loss distribution and that the actual areal fraction is most likely lower. Thus, Figure 7 demonstrates that the actual loss fraction is around a few percent and that the new methodolgy outlined in Section II gives reasonable estimates of losses unlike the front-foil noise correction. Additionally, poloidal and radial variation is now plainly evident which could have important physical meaning and elucidate new transport mechanics.

IV. CONCLUSION

A methodolgy was proposed for better characteriznig and correctinig the capacitive plasma pickup up noise in JET's Faraday cup lost alpha detector array. Mode resonant losses can be extracted from the Faraday foil spectrograms to give a more exact description of the losses in (frequency,time)-space. The deepest foil within a given Faraday stack is subtracted from the others as a noise correction. The fourth foil is only susceptible to very high energy particles which are often absent or minimal in number, so that the only signal remaining is the capacitive pickup signature. Comparing this post-processing methodology with that of using the front-foil as a corrective feature with simple band-pass filtering, one finds that the feature finding greatly reduces the measurement uncertainty while obtaining more accurate lost ion signal values.

Some key assumptions must be made in the post-processing analysis. Namely, that the capacitiive pickup among foils is approximately consistent among all foils in a stack and that the real losses on the fourth foil are negligible. Knowing the loss population would require verification of the energetic particle distribution function and its associated losses. This is a challenging task that requires detailed modeling so is not always pertinent when analyzing a large number of discharges. Obtaining a measurement of the exact plasma coupling is even harder and would require detailed modelling of the edge electric field. Additionally, the spectral feature finding method does not account for non-coherent losses. Therefore, hardware changes still remain the best path forward for mitigating the plasma capacitive pickup. Hardware changes can help eliminate the needed assumptions while providing further constraints on the measured signal. However, as machine access is limited and diagnostic upgrades occur infrequently, the bulk of noise characterization and correction must be done during post-processing analysis.

ACKNOWLEDGEMENTS

This manuscript is based upon work supported by the U.S. Department of Energy, Office of Science, Office of Fusion Energy Sciences, and has been authored by Princeton University under Contract Number DE-AC02-09CH11466 with the U.S. Department of Energy. This work has been carried out within the framework of the EUROfusion Consortium, funded by the European Union via the Euratom research and training programme (Grant Agreement No 101052200 - Eurofusion). Views and opinions expressed are however those of the author(s) only and do not necessarily reflect those of the European Union or the European Commission. Neither the European Union nor the European Commission can be held

responsible for them.

The work of all JET task force leaders, scientific coordinators, and diagnosticians is also greatly appreciated.

The data that support the findings of this study are available from the corresponding author upon reasonable request.

[1] S. E. Sharapov, B. Alper, D. Borba, L. G. Eriksson, A. Fasoli, R. D. Gill, A. Gondhalekar, C. Gormezano, R. F. Heeter, G. T. A. Huysmans, *et al.*, Nucl. Fusion **40**, 1363 (2000).
[2] R. J. Dumont *et al.*, Nucl. Fusion **58**, 082005 (2018).
[3] L. Garzotti *et al.*, Nucl. Fusion **59**, 076037 (2019).
[4] R. Dumont *et al.*, "Scenario preparation for the observation ofalpha-driven instabilities and transport of alpha particles in JET DT plasmas. FEC IAEA 2020 - 28th IAEA Fusion Energy Conference, May 2021, Nice (E-Conference), France.".
[5] J. Mailloux *et al.*, "*Nucl. Fusion*, Overview of JET results for optimising ITER operation," (Accepted 2022).
[6] D. S. Darrow, A. Werner, and A. Weller, Rev. Sci. Instrum. **72**, 2936 (2001).
[7] D. S. Darrow, S. Baumel, F. E. Cecil, V. Kiptily, R. Ellis, L. Pedrick, and A. Werner, Rev. Sci. Instrum. **75**, 3566 (2004).
[8] D. S. Darrow, Rev. Sci. Instrum. **79**, 023502 (2008).
[9] M. Garcia-Munoz, H. U. Fahrbach, H. Zohm, and ASDEX Upgrade Team, Rev. Sci. Instrum. **80**, 053503 (2009).
[10] R. K. Fisher, D. C. Pace, M. Garcia-Munoz, W. W. Heidbrink, C. M. Muscatello, M. A. Van Zeeland, and Y. B. Zhu, Rev. Sci. Instrum. **81**, 10D307 (2010).
[11] M. Garcia-Munoz *et al.*, .
[12] P. J. Bonofiglo *et al.*, Nucl. Fusion **62**, 026026 (2022).
[13] D. S. Darrow, S. Baumel, F. E. Cecil, R. Ellis, K. Fullard, K. Hill, A. Horton, V. Kiptily, L. Pedrick, *et al.*, Rev. Sci. Instrum. **77**, 10E701 (2006).
[14] D. S. Darrow, F. E. Cecil, V. Kiptily, K. Fullard, A. Horton, A. Murari, and JET-EFDA Contributors, Rev. Sci. Instrum. **81**, 10D330 (2010).
[15] S. Yamamoto, K. Ogawa, M. Isobe, D. S. Darrow, S. Kobayashi, K. Nagasaki, H. Okada, T. Minami, S. Kado, S. Ohshima, *et al.*, Rev. Sci. Instrum. **87**, 11D818 (2016).
[16] S. Lazerson, R. Ellis, C. Freeman, J. Ilagan, T. Wang, L. Shao, N. Allen, D. Gates, and H. Neilson, Rev. Sci. Instrum. **90**, 093504 (2019).
[17] S. Baeumel, A. Werner, R. Semier, S. Mukherjee, D. S. Darrow, R. Ellis, F. E. Cecil, L. Pedrick, H. Altmann, and V. Kiptily, Rev. Sci. Instrum. **75**, 3563 (2004).
[18] F. E. Cecil, V. Kiptily, A. Salmi, A. Horton, K. Fullard, A. Murari, D. Darrow, K. Hill, and JET-EFDA Contributors, Rev. Sci. Instrum. **81**, 10D326 (2010).
[19] F. E. Cecil, V. Kiptily, D. S. Darrow, A. Murari, and J.-E. Contributors, Nucl. Fusion **52**, 094022 (2012).
[20] P. J. Bonofiglo, V. Kiptily, A. Horton, P. Beaumont, R. Ellis, F. E. Cecil, M. Podesta, and J. Contributors, Rev. Sci. Instrum. **91**, 093502 (2020).
[21] D. R. Ferreira, T. A. Martins, P. Rodrigues, and JET Contributors, Mach. Learn: Sci. Technol. **3**, 015015 (2022).
[22] B. Joshua, G. Marina, P. Francesca, S. Jai, P. Alexei, and P. Gopan, "2018 *TRANSP Software* USDOE Office of Science (SC), Fusion Energy Sciences (FES) (https://doi:10.11578/dc.20180627.4),".
[23] www-nds.iaea.org/.
[24] A. Pankin *et al.*, Commput. Phys. Commun. **159**, 157 (2004).
[25] M. Brambilla *et al.*, Plasma Phys. Control Fusion **41**, 1 (1999).
[26] C. Di Troia, Plasma Phys. Control. Fusion **54**, 105017 (2012).
[27] C. Di Troia, Nucl. Fusion **55**, 123018 (2015).
[28] V. G. Kiptily *et al.*, Plasma Phys. Control. Fusion **64**, 064001 (2022).
[29] A. Fasoli *et al.*, Nucl. Fusion **36**, 258 (1996).